Bull. Fish. Sci. Hokkaido Univ.
55(1), 53-62, 2004.

Spatial Distribution of Diffusive Type Fine Structure Observed on 26.7-27.2σ_θ Surfaces in the Gulf of Alaska

Yutaka ISODA[1], Shogo TAKAGI[2], Akinori MURATA[2] and Noriyuki SUGAWARA[2]

(Received 27 February 2004, Accepted 2 June 2004)

Abstract

A diffusive type fine structure with several temperature inversions has often been observed on the 26.7-27.2σ_θ surfaces in the Gulf of Alaska, which have an approximate density range of North Pacific Intermediate Water (NPIW). In order to examine the possible cause of such a fine structure, hydrographic observations in the eastern North Pacific subarctic region were carried out in June-July 1995, 1996, and 1997. Hydrography in the Gulf of Alaska confirmed the existence of the diffusive type fine structure below another diffusive domain, which has an intense temperature inversion confined to a strong halocline with a lighter density range of 25.8-26.5σ_θ. Our focused diffusive type fine structure was zonally distributed, at least from 145°W to 180° along almost the same density range of 26.7-27.2σ_θ. Hydrography in the meridional transect of 180° suggests that a significant diffusive double-diffusion process, which occurred around the Subarctic Front at a nearly NPIW density of 26.8σ_θ, may be responsible for the additional ventilation site of NPIW. From the spatial distribution of such a diffusive domain, it is inferred that a cross-gyre flow from the subtropical region east of Japan to the Gulf of Alaska (Ueno and Yasuda, 2000), where the heat can be continuously supplied from densities greater than 26.8σ_θ, contributes to the maintenance and transport of diffusive type water masses along the NPIW density range.

Key words: diffusive type, Hydrography, Gulf of Alaska, NPIW density range

Introduction

The North Pacific Intermediate Water (NPIW) is characterized as a salinity minimum that coincides with the 26.7-26.9σ_θ density range, and extends to the subtropical gyre. Several alternative processes for the NPIW formation have been proposed. According to recent studies (Riser and Swift, 1989; Talley, 1991, 1993, 1997; Talley et al., 1995; Yasuda et al., 1996 and Yasuda, 1997), the NPIW represents the extent of ventilation in the North Pacific, and has its source in the western North Pacific subarctic region as the only site. Talley (1991) proposed that the relevant processes include sea ice formation in the Okhotsk Sea, and vertical mixing primarily in the Kuril Straits. Yasuda (1997) suggested that the origin of the NPIW is the Okhotsk Sea Mode Water with the characteristics of low potential vorticity, and that its part flows southward along the Japanese islands with a form of density-driven current. However, Van Scoy et al. (1991) proposed that the Gulf of Alaska might be an additional ventilation site of NPIW from hydrographic and tritium data analysis. They suggested that an evaluation of the energy stored in the water column and of the wind and buoyancy forcing shows that during winter conditions, enough energy can be pumped into the system to force 26.8σ_θ to outcrop in the Gulf of Alaska.

Recently, You et al. (2000) examined the role played by the Alaskan Gyre, and proposed two different NPIW formation sources in the North Pacific, one in the Alaskan Gyre characterized by high potential vorticity on a 26.5σ_N (neutral surface), and the other in the Okhotsk Sea, characterized by low potential vorticity on 27.2σ_N and 27.4σ_N. They also showed that the NIPW supplied from the Alaskan Gyre contributes in the eastern part of the subtropical gyre east of the date line. Such formation and circulation of the NPIW were inferred by the existence of apparent diffusive double-diffusion estimated from the Turner angle calculations. Then the estimated circulation in the eastern part mainly occurs at densities $<26.8\sigma_N$; hence its density is slightly lower than that of the western NPIW, whose origin is the Okhotsk Sea.

However, the existence of another temperature inversion in the density range of 26.8-27.25σ_θ within the Gulf of Alaska is also an observational fact (Musgrave et al.,

[1] *Laboratory of Marine Environmental Science, Graduate School of Fisheries Sciences, Hokkaido University*
(e-mail: isoda@sola3.fish.hokudai.ac.jp)
(北海道大学大学院水産科学研究科資源環境科学講座)
[2] *Faculty of Fisheries, Hokkaido University*
(北海道大学水産学部)

1992). Its density range is rather close to that of the western NIPW. That is, there are two types of diffusive temperature inversions in the Gulf of Alaska. Musgrave et al. (1992) showed that the lighter/shallower inversion is located in the strong halocline, hence with high potential vorticity, while the heavier/deeper inversion is located in the sub-halocline. They proposed two mechanisms of the heavier/deeper temperature inversions around the $26.8\sigma_\theta$ surface; one due to wind mixing by intense winter storms, which was originally proposed by Van Scoy et al. (1991), and the other due to subsequent lateral/isopycnal mixing by mesoscale eddy activity within the Gulf. From these observation results of Van Scoy et al. (1991) and Musgrave et al. (1992), we see a modification of new water to the NPIW layer in the Gulf of Alaska, but the process by which this occurs is still unclear. The main objectives of the present study are to investigate the spatial distribution of the diffusive type fine structure in the NPIW density range, utilizing CTD (salinity, temperature and pressure) data, and to discuss its origin and modification process.

In this paper, the observations and the analysis method are explained in the 2nd section, and the vertical distributions of hydrographic properties (temperature, salinity, density, potential vorticity, and the diapycnal mixing parameter of the Turner angle) in the eastern North Pacific in 1995 are described in the 3rd section. In the Gulf of Alaska, two types of diffusive double-diffusion with temperature inversions were clearly found in two separate density ranges. The shallower diffusive domain occurred in the density range of $25.8\text{-}26.5\sigma_\theta$, as suggested by You et al. (2000). The fine structure with several temperature inversions on the $26.7\text{-}27.2\sigma_\theta$ surfaces, suggested by Musgrave et al. (1991), was zonally distributed from 145°W to 180°. In the 4th section, the interannual variabilities of the above hydrographic properties are investigated by using the CTD data in 1996 and 1997. The spatial changes of temperature inversions on the $26.7\text{-}27.2\sigma_\theta$ surfaces, according to the anti-clockwise general circulation in the eastern North Pacific, are examined in the 5th section. The possible process that occurs to make such a fine structure is directed to the lateral intrusion of warm and salt cross-gyre waters from the western subtropical gyre at densities greater than $26.8\sigma_\theta$ into a cold and low-salinity subarctic water. The relationship between our results and the previous studies are discussed in the final section.

Data and Methods

The CTD data used for the present analyses are hydrographic measurements taken on a cruise on board the T/S *Oshoro-maru* in June-July 1995, 1996, and 1997. The CTD instrument used was a Neil Brown Mark III. Vertical CTD profiles were taken along the following three observation lines in the eastern North Pacific subarctic region: 180°, and around 160°W and 145°W (see Fig. 1). Thirty-five (1-35: 180°), ten (1-

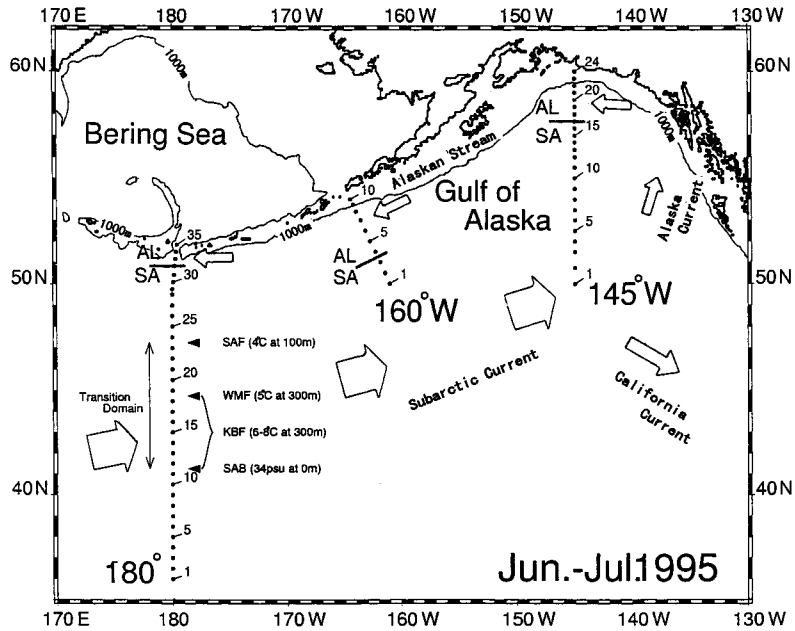

Fig. 1. The cruise track on board the T/S *Oshoro-maru* in June-July 1995. It consisted of three observation lines in the eastern North Pacific: 180°, around 160°W and 145°W. The general circulation in this area has an anti-clockwise current system, as schematically shown by the white arrows, i.e., the Subarctic Current (SA), the Alaska Current, and the Alaskan Stream (AL). The four major fronts in the SA are the Subarctic Front (SAF), the Water Mass Front (WMF), the Kuroshio Bifurcation Front (KBF), and the Subarctic Boundary (SAB).

10: around 160°W), and twenty-four stations (1-24: 145°W) were occupied on each line running from south to north. Since the CTD data in 1996 and 1997 were limited to two meridional transects of the 180° and 145°W lines, those are used for comparison with the data in 1995 to explore the possible effects of temporal variability on the present conclusions. Our cruise track at a 180° line was designed to cross the major fronts roughly perpendicular to the axes of the broad eastward flows; the Subarctic Front (SAF: the 4°C isotherm at 100 m depth) and the Subarctic Bounbary (SAB: 34 psu at 0 m), which were defined by Favorite et al. (1976). The zone between both fronts is called the Transition Domain. Several additional fronts within the Transition Domain have recently been identified. These fronts are the Water Mass Front (WMF: the 5°C isotherm at 300 m depth; Zhang and Hanawa (1993)) and the Kuroshio Bifurcation Front (KBF: the 6-8°C isotherm at 300 m depth; Mizuno and White (1983)). Here, the density gradient across the WMF is weak, because the changes in temperature and salinity are nearly density-compensating. The locations of their fronts in 1995 are plotted at the right hand side of the 180° stations. The cruise tracks at the 160°W and 145°W lines, however, were not completed to detect their fronts, and were situated just between the SAF and WMF.

In the vertical density distributions which are discussed later in Figs. 2c, 3c, and 4c, we can find the intense narrow westward flow along the northern most boundary. This flow is called the Alaskan Stream (AL), and behaves like a western boundary current (Royer and Emery, 1987; Warren and Owers, 1988). The origin of the AL is its southern broad eastward flow of the Subarctic gyre (SA) or Subtropical gyre (ST), as schematically shown by the white arrows in Fig. 1. The solid lines plotted at each line mark the boundary between the SA and AL in 1995.

Vertical profiles of the potential temperature (θ) and salinity (S) were measured from the sea surface down to the sea bottom or the maximum pressure of 3,000 dbar. The raw CTD data were averaged to the 1-dbar intervals, and 1-dbar data were smoothed by the five times operation of $[A_{i-1}+2A_i+A_{i+1}]/4$ (A_i represents a water property at i-th pressure), applying the method

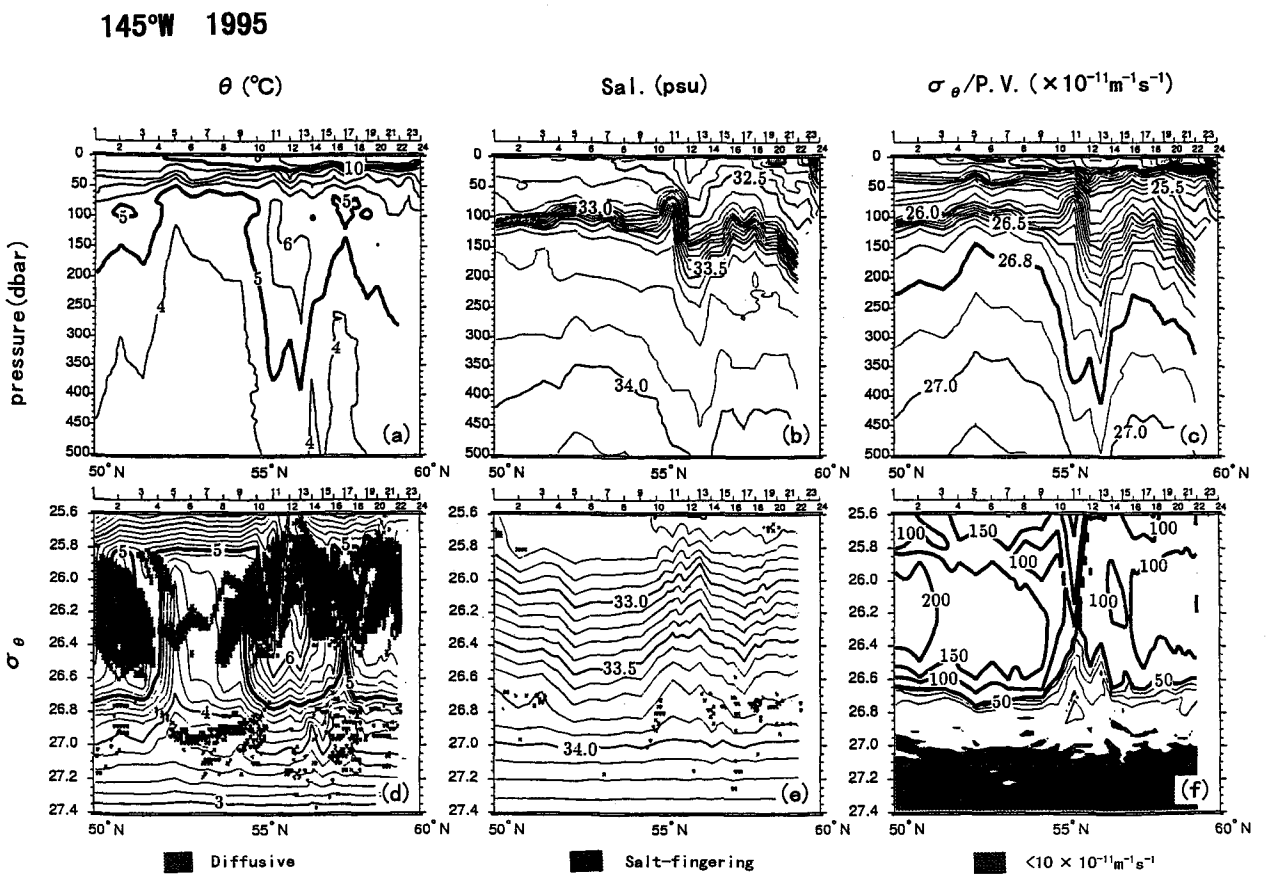

Fig. 2. The vertical distributions from the 1995 CTD cruise at the 145°W line: (a) potential temperaure: θ vs pressure, (b) salinity: S vs pressure, (c) potental density: σ_θ vs pressure, (d) θ vs σ_θ, (e) S vs σ_θ, and (f) potential vorticity: P.V. vs σ_θ. The water favorable for "diffusive" and "salt-fingering", respectively, is superimposed on (d) θ vs σ_θ, (e) S vs σ_θ as shaded marks. The layer with P.V. less than 10×10^{-11} m^{-1} s^{-1} is shaded on (f) P.V. vs σ_θ.

developed by Yasuda et al. (1996). To investigate the water-mixing process, we estimated the Turner angle (T_u), which is the parameter indicating the relative strength of double-diffusion. According to Ruddick (1983), T_u is given by

$$T_u=\tan^{-1}(-R_\rho)-45^\circ$$
$$R_\rho=\alpha\theta_Z/\beta S_Z$$

where the non-dimensional parameters R_ρ indicates the density ratio, $\alpha=-\rho^{-1}\partial\rho/\partial\theta$ and $\beta=\rho^{-1}\partial\rho/\partial S$ (ρ is a water density) are expansion coefficients for temperature (θ) and salinity (S), respectively. θ_Z and S_Z are the vertical temperature and salinity gradients, respectively. T_u in degrees represents "diffusive" double-diffusion for $-90^\circ<T_u<-45^\circ$, "salt-fingering" double-diffusion for $45^\circ<T_u<90^\circ$ and doubly stable for $|T_u|<45^\circ$, which means the water column is stably stratified with respect to both the temperature and salinity. Therefore, the fine structure with temperature inversion can be found by the "diffusive" double-diffusion.

It has been known that low potential vorticity is a useful indicator for identifying the ventilation source of water masses in winter, or the conservative property independent of temperature and salinity (Talley, 1988; Yasuda, 1997). On the basis of the potential vorticity distribution along a particular density surface in the Pacific Ocean, You et al. (2000) found that there are two different NPIW formation sources: one in our study area, i.e. the Gulf of Alaska, which is characterized by high potential vorticity, and the other in the Okhotsk Sea, characterized by low potential vorticity. We used the following potential vorticity (Q), neglecting the relative vorticity, as defined by Yasuda(1997).

$$Q=f\rho^{-1}\partial\sigma_\theta/\partial z$$

where f is the Coriolis frequency, and z is a vertical axis. For the estimation of $\partial\sigma_\theta/\partial z$, the density gradient was calculated as a least mean square of the 50-dbar data for each smoothed 1-dbar interval.

Hydrographic Structures in 1995

In the following three observation lines (Figs. 2, 3, and 4), hydrographical transects are presented for the north-south segments to delineate the dynamical features of the eastern North Pacific in summer. These figures are drawn with the following same manners; the upper three panels show the vertical distributions of (a) potential temperature: θ, (b) salinity: S and (c) potential density: σ_θ from the 0 to 500 dbar, and the

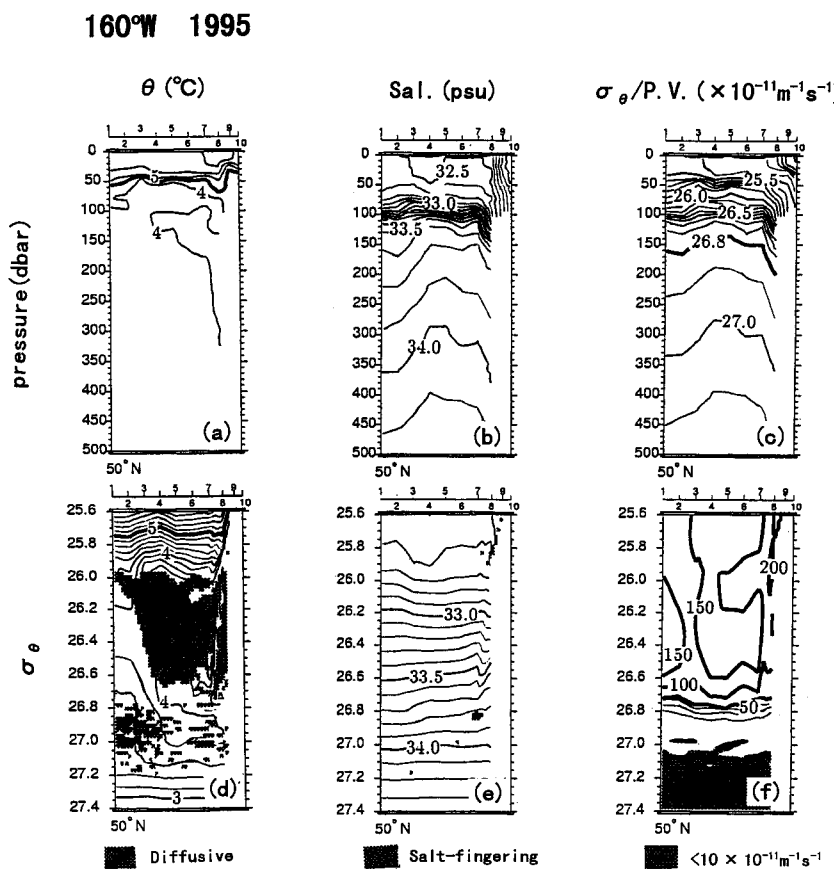

Fig. 3. Same as Fig. 2, except for the CTD cruise around the 160°W line.

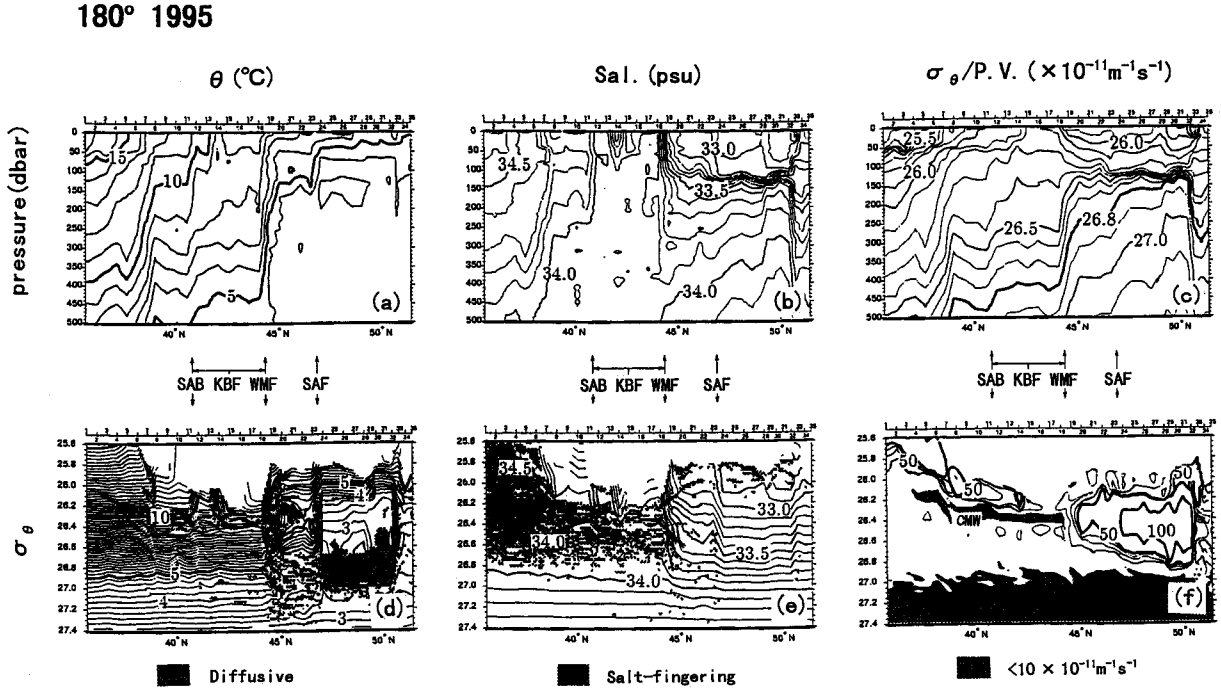

Fig. 4. Same as Fig. 2, except for the CTD cruise at the 180° line.

lower three panels show the (d) θ, (e) S and (f) potential vorticity: P.V. plotted with density: σ_θ as the ordinate. The water favorable for "diffusive" and "salt-fingering", respectively, is superimposed on (d) θ vs σ_θ and (e) S vs σ_θ property distributions as the shaded marks.

Hydrography at the 145°W Line within the Gulf of Alaska

There are two distinct pycnoclines in the upper 200 dbar; one is formed by the thermocline at the 20-50 dbar, and the other is formed by the halocline at the 100-200 dbar (Figs. 2a-c). It was also found that the temperature minimum/maximum, i.e., a temperature inversion, extends above/below the halocline at Stn. 1-4 and Stn. 10-22. A most significant temperature maximum (>6°C) appears within an anticyclonic eddy located around 55°N (Stn. 10-16). The occurrence of this eddy has been mentioned previously (Tabata, 1967; Tabata, 1982; Onishi et al., 2000), and the eddy is often called the "Sitka" eddy. The water at the center of the eddy in the layers from 100 dbar to at least 500 dbar is warmer and less saline than at corresponding depths away from the center. Such temperature inversions can be seen as the diffusive double-diffusion within a high potential vorticity more than 100×10^{-11} m^{-1} s^{-1} at the density range of 25.8-26.5σ_θ (Figs. 2d, 2f).

As a possibility for the formation process of the above temperature inversion, warming in summer forms a seasonal thermocline above a temperature minimum layer, and the temperature minimum water will be a winter-water formed by preceding winter cooling, reflecting its origin in the surface mixed layer above the strong halocline. It is known that the existence of this temperature maximum below the halocline might be the cause of a pure seasonal cycle suggested by Ueno and Yasuda (2000). That is, in spring and summer, a temperature maximum exists at around 100 dbar, while in fall, at the end of the heating period, it vanishes.

The water favorable for diffusive double-diffusion is also found on the higher 26.8σ_θ surface, except for a small area near the Sitka eddy which shows a little salt-fingering (Figs. 2d, 2e). This deeper diffusive domain corresponds to the fine structure with several temperature inversions, as pointed out by Musgrave et al. (1992). Its density range is much too heavy to be directly affected by the shallower diffusive double-diffusion on 25.8-26.5σ_θ, and the water has a much lower potential vorticity less than $10\text{-}50\times10^{-11}$ m^{-1} s^{-1}, colder θ=3-4°C and saline S=33.8-34.2 psu (Fig. 2f). The differences in water properties between the shallower and deeper diffusive domains reflect different formation mechanisms and circulation histories.

Hydrography at the 160°W Line

As a whole, the distributions for two types of diffusive double-diffusion waters shown in Fig. 3 are similar to those at the 145°W line in the Gulf of Alaska. In the shallower diffusive domain, however, its temperature range of about 4°C is somewhat colder than that of

about 5°C at 145°W, and its density range of 26.0-26.7σ_θ is heavier than that of 25.8-26.5σ_θ at 145°W. In the deeper diffusive domain, on the other hand, the water properties (θ=3-4°C, S=33.8-34.2 psu), density (σ_θ= 26.8-27.2), and potential vorticity (P.V.=10-50$\times 10^{-11}$ m^{-1} s^{-1}) ranges are almost the same as those at 145°W in the Gulf of Alaska.

Hydrography at the 180° Line

The Alaskan Stream (AL), characterized by a lower salinity water, is observed at the northern boundary as a narrow band (Figs. 4b, c). The significant WMF around 45°N clearly marked the southern limit of waters with surface lower salinity, and indicated the change from the subtropical and subarctic water masses in the subsurface layer. The region that lies between SAB at 41°N and WMF at 45°N is composed of uniform salinity water with 33.9-34.0 psu (Fig. 4b). Then, the water south of SAB has a subsurface salinity minimum. This water at the salinity minimum is called the NPIW. As noticed by many previous investigators, the core of the salinity minimum resides on the isopycnal surface of 26.8σ_θ ; therefore, the water favorable for salt-fingering is widely distributed on a lighter density <26.8σ_θ south of SAB (Fig. 4e).

Another interesting water mass in the central subtropical region is the Central Mode Water (CMW : Roden (1980)). The CMW characterized by low potential vorticity P.V.$<10\times 10^{-11}$ m^{-1} s^{1-}, i.e. pycnostads or mode waters, extends on the 26.2-26.4σ_θ to the south of WMF or KBF, and likely corresponds to weak diffusive double-diffusion (Figs. 4d and 4f). Recently, Suga et al. (1997) showed that the CMW is formed by wintertime deep convection due to surface cooling, and spreads from its formation area around KBF at 175°E-160°W as far south as about 37°N around 170°E by lateral advection. Therefore, the water below CMW cannot outcrop in the surface, so that the existence of NPIW below CMW, observed at 180°, reflects the eastward advection from the upstream area along the 26.8σ_θ surface.

In the region between WMF and SAF, the marked temperature inversions denoted by the diffusive domain are found on the 26.7-27.2σ_θ surface (Fig. 4d). In this line, the shallower temperature inversion within a high potential vorticity at the lighter density range <26.7σ_θ is not observed. Vertical characteristics of temperature inversion are found at the heavier density range >26.7 σ_θ, and are closely related to the strength of the halocline. The largest potential vorticity P.V.$>100\times 10^{-11}$ m^{-1} s^{-1} north of SAF at 47°N is formed according to the strong halocline, and this P.V. value on the isopycnals around 26.8σ_θ decreases southward to the WMF (Fig. 4f). The diffusive domain between WMF and SAF locates that a lower potential vorticity less than P.V.$<$ 50×10^{-11} m^{-1} s^{-1} accompanies several fine temperature inversions, while that north of SAF has a pair of single temperature minimum (2.6-3.0°C, ~26.7σ_θ) within the high potential vorticity P.V.$>100\times 10^{-11}$ $m^{-1}s^{-1}$ and single temperature maximum (~3.4°C, ~27.0σ_θ) with P.V.$<10\times 10^{-11}$ $m^{-1}s^{-1}$ (Figs. 4d, f). The latter temperature inversion profile versus density is consistent with the characteristics of a typical subarctic water mass in the western North Pacific, as defined by Zhang and Hanawa (1993), although the temperature minimum/maximum density and temperature are not exactly coincident. That is, the typical temperature minimum/maximum has 2.40°C on 26.6σ_θ and 3.55°C on 26.9σ_θ, respectively (from Table 1 of Zhang and Hanawa (1993)).

Hydrographic Structures in 1996 and 1997

We compared the 145°W (Fig. 5) and 180° (Fig. 6) meridional transects of 1996 and 1997 with the hydrographic properties in 1995 to explore the possible effects of temporal variability on the present conclusions. To confirm the density range of the diffusive type fine structure and its spatial extent, the potential temperature : θ (left panel), and potential vorticity : P.V. (right panel) distributions plotted with density : σ_θ as the ordinate are only shown. Their figures are drawn in

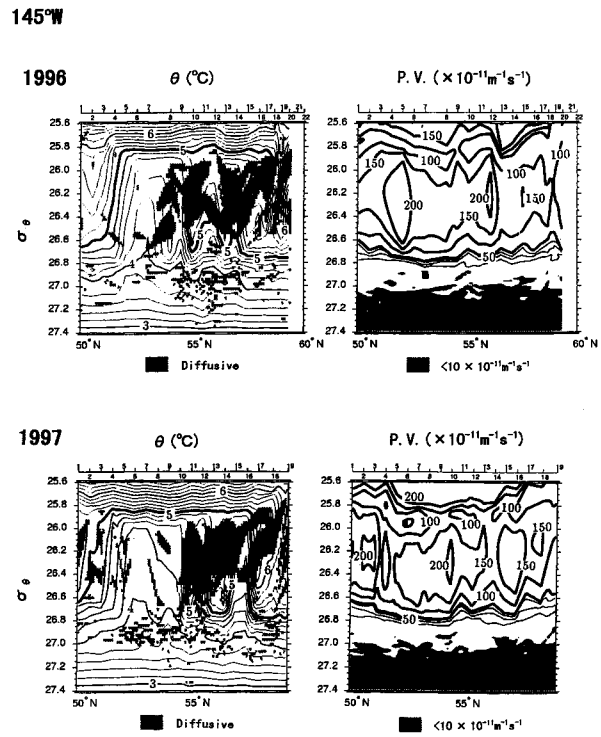

Fig. 5. Same as Figs. 2d (θ vs σ_θ) and 2f (P.V. vs σ_θ), except for the 1996 and 1997 CTD cruises at the 145°W line.

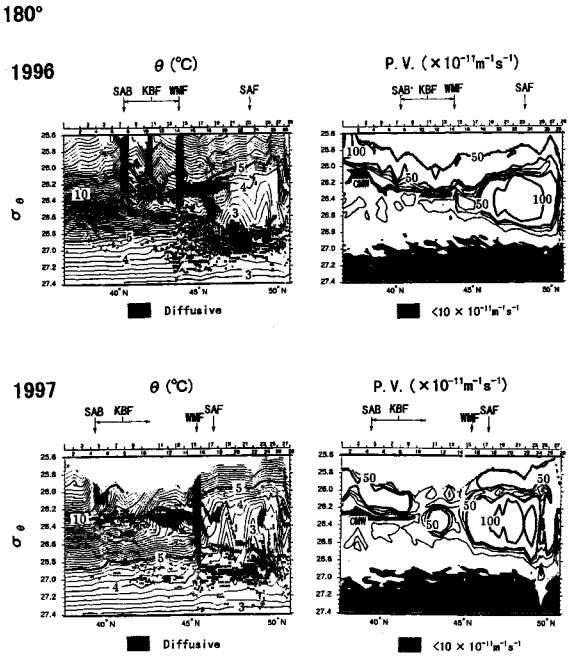

Fig. 6. Same as Fig. 4d (θ vs σ_θ) and 4f (P.V. vs σ_θ), except for the 1996 and 1997 CTD cruises at the 180° line.

the same manner as Figs. 2d, f, and 4d, f.

Hydrography at the 145°W Line

The southern boundary of the Alaskan Stream exited at 57°N in 1996, and at 57.5°N in 1997, and the northern boundary of the Subarctic Current exited at 52°N in both years. It was found that the Sitka eddy with a warm core has been located at around 55°N throughout three years (1995-1997), although the size of the eddy along the 145°W in 1996 and 1997 was somewhat smaller than it was in 1995 (Onishi et al., 2000). Two types of similar diffusive domains can be discerned in the Gulf of Alaska. One is the water property with a high temperature of $\theta \sim 5$°C and a high potential vorticity of P.V.$> 100\times10^{-11}$ m^{-1} s^{-1} in the density range of 25.8-26.6σ_θ, and the other is that with a temperature less than 4°C and a low potential vorticity of P.V.$\sim$10-20$\times10^{-11}$ m^{-1} s^{-1} in the NPIW density range of 26.8-27.2σ_θ.

Hydrography at the 180° Line

The WMF, which is the boundary between the SA and ST water masses, was located at 44°N in 1996 and at 46°N in 1997. The location of this WMF was close to that of KBF in 1996, but close to that of SAF in 1997. Despite the differences, due to interannual changes of the front locations, we found several features in common in the three-year cruises. For example, the CMW in the density range of 26.0-26.4σ_θ (the low potential vorticity area of P.V. $<10\times10^{-11}$ m^{-1} s^{-1}) is developed to the south of the KBF, and is accompanied by a weak temperature inversion. Another common feature is that the diffusive type fine structure occurs to the north of the WMF below 26.8σ_θ, with a lower potential vorticity less than P.V.$<50\times10^{-11}$ m^{-1} s^{-1}. Although the short distance between the WMF and SAF in 1997 may distort the spatial distribution of the diffusive temperature inversion, the presence of a single temperature maximum and minimum around SAF is relatively stable. The along-isopycnal potential vorticity between the 26.7-27.2σ_θ surface gradually transits from the north of the SAF with prominent temperature inversion to the WMF, where potential vorticity is mostly uniform and low.

Especially, the diffusive domain in 1996 clearly shows that the fine structure in the north of WMF below 26.8 σ_θ was formed below a weak temperature inversion along the nearly CMW density range. This suggests that some lateral process between WMF and SAF may be important to the formation of the diffusive type fine structure. However, it is unclear that how such fine structure will be able to coexist along the NPIW density range in both the 145°W and 180° transects, which is more than 3,000 km distant. This question is addressed in the following section.

Spatial Distribution of the Temperature Inversion on 26.7-27.2σ_θ in 1995

The temperature versus density plotted in Fig. 7 along the three observation lines in 1995 helps to verify the spatial extension of the temperature inversion for 26.7-27.2σ_θ. The upper and lower panels include data at stations of the AL and SA/ST regions, respectively (see Fig. 1). In the AL region, data at the stations with densities greater than 26.7σ_θ are only plotted. The schematic white arrows in Fig. 7 roughly indicate the anti-clockwise general flow pattern. In the SA/ST region at the 180° line, we excluded waters near WMF (stations 19 to 23) and defined the typical subarctic (SA) and subtropical (ST) waters by linearly connecting the modes on the isophycnal surfaces. The calculated two typical waters are plotted as thick solid lines in all panels.

The temperature between the SAF and WMF (stations 19 to 23) at the 180° line changed abruptly, accompanying the fine structure of several temperature inversions, although the distance is only about 20 km (Fig. 7d). Since the cruise tracks at the 160°W and 145°W lines were situated within an eastward flow region between SAF and WMF, we detected spatial changes of such temperature inversion along the downstream from west to east. The shaded areas in Figs. 7e and 7f indi-

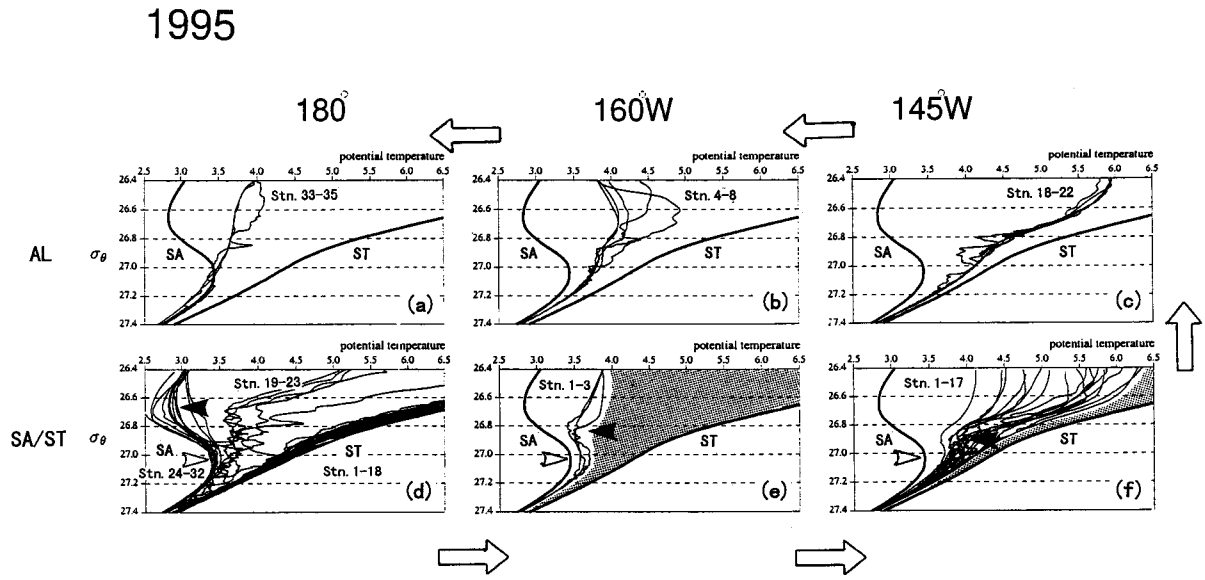

Fig. 7. Temperature vs density showing the occurrence of the fine structure at densities between 26.6 and 27.2σ_θ. The upper (a-c) and lower (d-f) panels include data at the stations of the AL and SA/ST regions, respectively. The solid curves indicate the two typical water masses, i.e., SA and ST, determined in the present study. The black and white small triangle arrows indicate the minimum and maximum of some temperature profiles in the lower panels, respectively. The schematic white arrows roughly show the anti-clockwise general flow pattern.

cate the expected temperature versus the density domain, if the CTD observations at the more southern region from the present observation lines of 160°W and 145°W will be carried out. The common feature in Figs. 7d-f is that the minimum and maximum of some temperature profiles, which are indicated by black and white small triangle arrows, are observed. However, their density and strength vary from line to line. The density range of the minimum increases eastward from 26.7σ_θ at 180° to 26.9σ_θ at 145°W, while the maximum occurs over a limited density range around 27.0σ_θ at three lines. Both the minimum and maximum values gradually increase eastward, and their strength in their temperature difference becomes weak.

Along the Alaskan Stream area (AL) in Figs. 7a-c, we found the highest temperature area at the 145°W line. Its temperature profile is close to that of subtropical water (Fig. 7c). The temperature in a wide density range uniformly decreases westward from 145°W to 180°. At the 160°W line, the range of temperature in the AL area (Fig. 7b) is rather higher than in its southern SA/ST area (Fig. 7e). At the 180° line, the temperature in the AL area is colder than the typical subarctic water (SA) for the density range >27.0σ_θ (Fig. 7a). This implies that this water may have exchanged with colder water in the Bering Sea.

Thus, the temperature inversion in 26.7-27.2σ_θ starts around the northern end of the WMF at 180°, and extends eastward throughout any diffusion process. We suspect that such diffusion processes are not only related to vertical turbulent mixing or double-diffusion, but also lateral water mixing between the subarctic and subtropical waters.

Summary and Discussion

In general, diffusive interfaces occur at the top and salt-fingering interfaces at the bottom of intruded warm saline layers. The balance between the two, similar to a sandwich structure due to a layered intrusion of contrasting water mass, will induce an effective diapycnal mixing. However, the overall mixing observed in the Gulf of Alaska was dominated only by diffusive mixing; therefore, active double-diffusion may not be expected there. It is inferred that these water masses have been mixing for a long time, thus reducing the potential for double-diffusion, and that diffusive mixing only remains.

In their diffusive mixings, the most vigorous potential for diffusive layers, i.e., an intense temperature inversion, was on the 25.8-26.5σ_θ surface. However, the formation process of this diffusive domain is not due to the lateral intrusion process. Warming in summer forms a seasonal thermocline above a temperature minimum layer, as shown in Figs. 2a and 2d. This minimum water is called remnant winter water and is maintained by the strong halocline, reflecting its origin in the deeper mixed layers formed by winter cooling.

In the present study, we focused on another diffusive mixing, which was observed in the NPIW density range

of 26.7-27.2σ_θ. This water mass has a fine structure with several temperature inversions. It is suggested that such temperature inversions may start around the northern end of the WMF at 180°, and extend to the Gulf of Alaska. The estimated eastward advection time between both regions is quite long, about three years (e.g. Ueno and Yasuda (2000)). It seems, nevertheless, possible to expect similarity for temperature inversion between the 180° and 145°W lines. These features imply that a large-scale background profile favorable to diffusive mixing exists in the eastern North Pacific subarctic region. That is, the fine structure observed at each line will be the evidence of continuous heat-forcing from densities greater than 26.8σ_θ. One candidate for this possible scenario is the existence of the "cross-gyre flow", recently proposed by Ueno and Yasuda (2000).

Ueno and Ysuda (2000) investigated the distribution and formation of the mesothermal structure, i.e. the temperature inversion, in the North Pacific region using climatological hydrographic data. They suggested that the heat and salt that maintain the mesothermal water and thus the halocline in the density range of 26.7-27.2 σ_θ are transported as a cross-gyre flow from the transition domain just east of Japan, where the waters are influenced by the subtropical gyre water mass, to the eastern subarctic region. The proposed mean path of the warm and saline cross-gyre flow at 180° is between 45°N and 46°N, which well coincides with the region between WMF and SAF in 1995. Thus, they indicated the route of cross-gyre flow into the Gulf of Alaska, but the mesothermal structure discussed by Ueno and Yasuda (2000) was only the shallower temperature inversion on the 25.8-26.5σ_θ surface. Presumably, the fine structure with several temperature inversions on the 26.7-27.2σ_θ surface could not be resolved or laterally averaged on the climatological hydrographic data. Conversely speaking, the spatial expanse of the observed fine structure on the 26.7-27.2σ_θ surface indirectly supports the existence of the cross-gyre flow. Thus, we consider that this cross-gyre flow contributes to the maintenance and transport of the diffusive water masses along the NPIW density range.

Finally, we will discuss the first origin of the diffusive type fine structure on the 26.7-27.2σ_θ surface. At the 145°W and 160°W lines, two types of diffusive domains are clearly found in two separate density ranges, while a heavier/deeper diffusive domain on the 26.7-27.2σ_θ surface is only observed around the SAF at the 180° line, except for around the CMW density range. It is suggested that the intense diffusive double-diffusion process around SAF at 180° brings subsurface cold low-salinity water down to the NPIW density, i.e., the possibility of additional ventilation of NPIW. Then, the diffusive type fine structure was frequently found between WMF and SAF, and its density range (26.7-27.2σ_θ) tends to be slightly heavier than that of intense temperature inversion around SAF (27.6-27.0σ_θ). From such increase of the density near the WMF, it is inferred that the first origin of a fine structure may be formed by cabbeling process during the lateral mixing of the cold fresh waters around SAF with the warm saline waters south of WMF. Using the tritium data, Van Scoy et al. (1991) indicated that the ventilation of NPIW may occur directly, at outcrops within the Gulf of Alaska. However, our observation results in 1995, 1996, and 1997 showed that such direct ventilation is not likely to occur there due to the existence of a lighter/shallower intense diffusive domain. The map for tritium distributions below 26.8σ_θ (Fig. 5 of Van Scoy et al. (1991)) shows that the highest tritium area zonally elongates from around 180° to the Gulf of Alaska. If the enhanced diffusive double-diffusion around SAF at 180° may be responsible for additional ventilation and such ventilated waters with a high-tritium may be continuously advected to the Gulf of Alaska by a cross-gyre flow, the observed tritium distributions can be also explained.

Acknowledgements

This work was supported by a Grant-in-Aid for Scientific Research on Salmon Ecosystems in the Gulf of Alaska (No. 11660174) from the Ministry of Education, Science, Sports and Culture, of Japan. The authors would like to thank Captain S. Yamaguchi and the officers and crew of the T/S *Oshoro Maru*, Hokkaido University, for their helpful support during the CTD observations. We also thank an referee for helpful comments on drafts of the manuscript.

References

Favorite, F., A.J. Dodimead, and K. Nasu (1976) Oceanography of the Subarctic Pacific region, 1960-71, *Bull. 33*, pp. 1-187, Int. North Pac. Comm., Vancouver, B.C., Canada.

Mizuno, K., and W.B. White (1983) Annual and interannual variability in the Kuroshio current system. *J. Phys. Oceanogr.*, **13**, 1847-1867.

Musgrave, D.L., T.J. Weingartner, and T.C. Royer (1992) Circulation and hydrography in the northwestern Gulf of Alaska. *Deep Sea Res., Part A*, **39**, 1499-1519.

Onishi, H., S. Ohtsuka and G. Anma (2000) Anticyclonic, baroclinic eddies along 145°W in the Gulf of Alaska in 1994-1999, *Bull. Fish. Sci. Hokkaido Univ.*, **51**, 31-43.

Ueno, H. and I. Yasuda (2000) Distribution and formation of the mesothermal structure (temperature inversions) in the North Pacific subarctic region. *J. Geophys. Res.*, **105**, 16885-16897.

Riser, S.C., and D.D. Swift (1989) Ventilation and North Pacific Intermediate Water formation in the Sea of Okhotsk. paper presented at the inagural meeting. Oceanogr. Soc., Monterey, Calif.

Roden, G.I. (1980) On the subtropical frontal zone north of Hawaii during winter. *J. Phys. Oceanogr.*, **10**, 342-362.

Royer, T.C., and W.J. Emery (1987) Circulation in the Gulf of Alaska, 1981. *Deep Sea Res., Part A*, **34**, 1361-1377.

Ruddick, B.R. (1983) A practical indicator of the stability of the water column to double-diffusive activity. *Deep Sea Res., Part A*, **30**, 1105-1107.

Suga, T., Y. Takei, and K. Hanawa (1997) Thermostad distribution in the North Pacific subtropical gyre: The Central Mode Water and Subtropical Mode Water. *J. Phys. Oceanogr.*, **27**, 140-152.

Tabata, S. (1967) Circulation of the northeast Pacific Ocean as deduced from isentropic analysis. Int. Assoc. Phys. Sci. Ocean, Proces-Verbaux No. 10, 14th General Assembly, Berne, 119-120.

Tabata, S. (1982) The anticyclonic, baroclinic eddy off Sitka, Alaska, in the northeast Pacific Ocean. *J. Phys. Oceanogr.*, **12**, 1260-1282.

Talley, L.D. (1991) An Okhotsk Sea anomaly: Implication for ventilation in the North Pacific, *Deep Sea Res., Part A*, **38**, S171-S190.

Talley, L.D. (1993) Distribution and formation of North Pacific Intermediate Water. *J. Phys. Oceanogr.*, **23**, 517-537.

Talley, L.D. (1997) North Pacific Intermediate Water transports in the mixed water region. *J. Phys. Oceanogr.*, **27**, 1795-1803.

Talley, L.D., Y. Nagata, M. Fujimura, T. Kono, D. Inagake, M. Hirai, and K. Okuda (1991) North Pacific Intermediate Water in the Kuroshio Oyashio mixed water region in spring, 1989. *J. Phys. Oceanogr.*, **25**, 475-501.

Van Scoy, K.A., D.B. Olson, and R.A. Fine (1991) Ventilation of North Pacific Intermediate Water: The role of the Alaska Gyre. *J. Geophys. Res.*, **96**, 16801-16810.

Warren, B.A., and W.B. Owens (1988) Deep currents in the Central Subarctic Pacific Ocean. *J. Phys. Oceanogr.*, **18**, 529-551.

Yasuda, I., K. Okuda, and Y. Shimizu (1996) Distribution and modification of North Pacific intermediate water in the Kuroshio-Oyashio interfrontal zone. *J. Phys. Oceanogr.*, **26**, 448-465.

Yasuda, I. (1997) The origin of the North Pacific Intermediate Water. *J. Geophys. Res.*, **102**, 893-909.

You,Y., N. Suginohara, M. Fukasawa, I. Yasuda, I. Kaneko, H. Yoritaka, and M. Kawamiya (2000) Roles of the Okhotsk and Gulf of Alaska in forming the North Pacific Intermediate Water. *J. Geophys. Res.*, **105**, 3253-3280.

Zhang, R.C., and K. Hanawa (1993) Features of the Water Mass Front in the northwestern North Pacific. *J. Geophys. Res.*, **98**, 967-975.